

# Seismic motion incoherency effects on soil-structure interaction (SSI) response of nuclear power plant buildings

Dan M. Ghiocel

*Ghiocel Predictive Technologies, Inc., New York, USA*

**ABSTRACT:** The paper discusses key aspects of stochastic modeling of seismic motion incoherency and its implementation in the context of current structural design practice for nuclear structures that incorporates the soil-structure interaction effects. The paper briefly describes the theoretical basis of stochastic and deterministic incoherent SSI approaches. It should be noted that these incoherent SSI approaches have been validated by two EPRI studies (Short, Hardy, Mertz and Johnson, 2006, 2007), being accepted by nuclear industry and US NRC for application to the seismic analysis of new nuclear power plant structures within the United States. Currently, these incoherent SSI approaches are used by Westinghouse for the seismic design of the AP1000 nuclear complex (Ghiocel, Li, Coogler and Tunon-Sanjur, 2009). The paper illustrates the effects of stochastic ground motion incoherency on seismic SSI responses for a typical nuclear reactor building with no mass eccentricity and a nuclear complex building with significant mass eccentricities founded on a rock site.

## 1 INTRODUCTION

### 1.1 Stochastic Modeling Terminology

Typically, the term “stochastic process” is used in conjunction with the time evolution of a dynamic random phenomenon, while the term “stochastic field” is used in conjunction with the spatial variation of a stochastic (hyper) surface. A space-time stochastic process is a stochastic function having time and space as independent arguments. The term “space-time stochastic process” is synonymous with the term “time-varying stochastic field.” Stochastic field term fits well with stochastic boundary value problems, including the problem of the seismic free-field motion local spatial variation within dense arrays of recorders.

Stochastic fields can be homogeneous or non-homogeneous, isotropic or anisotropic, depending on whether their statistics are invariant or variant to the axis translation and, respectively, invariant or variant to the axis rotation in space. It should be noted that the stochastic field models proposed by Abrahamson (Abrahamson, 2005, 2006, 2007) for approximating the local spatial variation of seismic motions assume an isotropic stochastic field model that is invariant to

translation and rotation in the horizontal ground surface plane.

For a seismic wave stochastic field, with an amplitude denoted  $u(t)$  in time domain and  $U(\omega)$  in frequency domain, the (pair) cross-spectral density (CSD) function for two separated locations on ground surface  $j$  and  $k$ ,  $S_{U_j, U_k}(\omega)$ , is expressed by

$$S_{U_j, U_k}(\omega) = [S_{U_j, U_j}(\omega)S_{U_k, U_k}(\omega)]^{1/2} \Gamma_{U_j, U_k}(\omega) \quad (1)$$

where  $S_{U_j, U_j}(\omega)$  and  $S_{U_k, U_k}(\omega)$  are the power spectral density (PSD) of the seismic motion at locations  $j$  and  $k$ , and  $\Gamma_{U_j, U_k}(\omega)$  is the pair coherence function for locations  $j$  and  $k$ .

More generally, the CSD function is a complex quantity. However, in many advanced engineering applications, since coherence function is assumed to be a real and positive quantity - this is used for quadrant symmetric and isotropic stochastic fields (Vanmarcke, 1983) - the CSD function is also real and positive. The coherence function,  $\Gamma_{U_j, U_k}(\omega)$ , is a measure of the similarity of the two location motions

including both the amplitude spatial variation and the wave passage effects.

The coherence function is a complex quantity, often called in earthquake engineering literature the “un-lagged” coherence function (Abrahamson, 2005, 2006, 2007). However, often in earthquake engineering practice, we use isotropic, “lagged” coherence functions that are real and positive quantity that incorporate only the amplitude spatial randomness effects with no consideration of the wave-passage effects. The numerical investigations shown in this EPRI report are based on “lagged” coherency models that consider only amplitude randomness aspects and neglect wave-passage aspects.

Inverting equation 1, we get the definition of the coherence function between two arbitrary motions:

$$\begin{aligned} \Gamma_{U_j, U_k}(\omega) &= \frac{S_{U_j, U_k}(\omega)}{[S_{U_j, U_j}(\omega)S_{U_k, U_k}(\omega)]^{1/2}} \\ &= \frac{E[U_j(\omega)U_k(\omega)]}{\{E[U_j(\omega)U_j(\omega)]E[U_k(\omega)U_k(\omega)]\}^{1/2}} \end{aligned} \quad (2)$$

In equation 2 using the statistical expectation operator, denoted by  $E[.]$ , we highlight that the CSD function,  $S_{U_j, U_k}(\omega)$ , at each frequency is identical with the second-order statistical moment (scaled covariance) of the motion amplitudes  $U_j(\omega)$  and  $U_k(\omega)$  assumed to be two random variables.

The last expression of coherence function in equation 2 (right-side term) at any given frequency is identical with the expression of a statistical correlation coefficient between two random variables that can be found in any statistical textbook. This observation suggests that a series of efficient engineering numerical tools developed for digital simulation of (static) stochastic spatial variation fields based on factorization of covariance kernels could be extended for simulation of seismic motion spatial variation fields using factorization of coherence kernels at each frequency.

### 1.2 Factorization of Coherency Kernels

Several factorization techniques can be used for simulating of complex pattern stochastic fields. A quite frequent approach in engineering research literature is to employ the Pearson differential equation for defining different types of stochastic series representations based on orthogonal Hermite, Legendre, Laguerre, and Chebyshev polynomials. These

polynomial expansions are usually called Askey chaos series.

A major application of stochastic field decomposition theory is the representation of stochastic fields using the covariance kernel factorization. These covariance-based techniques have a large potential for practical engineering applications because they can be applied to any complex, static, or dynamic Gaussian or non-Gaussian stochastic field.

There are two competing stochastic simulation techniques using the covariance kernel factorization: (1) Choleski factorization and (2) Spectral factorization (called sometime Karhunen-Loeve expansion, or POD expansion) based on eigen-decomposition.

Both techniques can be employed to simulate both static and dynamic stochastic fields including seismic incoherent motions. A notable property of these two simulation techniques is that they can handle both real-valued and complex-valued covariance kernels. For simulating space-time processes (or dynamic stochastic fields), both covariance-based techniques can be employed.

It should be noted that spectral factorization has the advantage of providing useful engineering insights. The covariance eigenvectors, also called spatial modes, describe the “wavelength” component structure of the stochastic spatial variation field. It should be noted that for random spatial variations with large correlation-lengths, the number of (covariance) spatial modes required by the stochastic field eigen-series expansion convergence is reduced to only few modes. This provides often practical advantages.

## 2 SEISMIC SSI ANALYSIS METHODOLOGY

The implementation of incoherent SSI analysis is based on the spectral factorization of the coherency kernel at each selected frequency. The seismic incoherent SSI analysis methodologies that are described below were implemented in the ACS SASSI code (Ghiocel, 2007, Short, Hardy, Mertz and Johnson, 2006, 2007) that is currently used for SSI analysis of a number of nuclear power plants in US and overseas.

In this section the basic stochastic modeling equations are described using the same notations used by Tseng and Lilhanand (Tseng and Lilhanand, 1997). The main differences in notation are that for structure dofs we use superscript  $s$  instead of subscript  $s$ ,

and for ground motion at interaction nodes we use superscript g instead of subscript g.

Let's consider first the free-field motion.

The coherent free-field motion at any interaction node dof k,  $U_k^{g,c}(\omega)$ , is computed by:

$$U_k^{g,c}(\omega) = H_k^{g,c}(\omega)U_0^g(\omega) \quad (3)$$

where  $H_k^{g,c}(\omega)$  is the (deterministic) complex coherent ground transfer function vector at interface nodes and  $U_0^g(\omega)$  is the complex Fourier transform of the control motion.

Similarly, the incoherent free-field motion at any interaction node dof k,  $U_k^{g,i}(\omega)$ :

$$U_k^{g,i}(\omega) = \tilde{H}_k^{g,i}(\omega)U_0^g(\omega) \quad (4)$$

where  $\tilde{H}_k^{g,i}(\omega)$  is the (stochastic) incoherent ground transfer function vector at interaction node dofs and  $U_0^g(\omega)$  is the complex Fourier transform of the control motion.

The main difference between coherent and incoherent free-field transfer function vectors is that the  $H_k^{g,c}(\omega)$  is deterministic quantity while  $\tilde{H}_k^{g,i}(\omega)$  is a stochastic quantity (tilde hat marks this) that includes deterministic effects due to the seismic plane-wave propagation, but also stochastic effects due to incoherent motion spatial variation in horizontal plane. Thus, the incoherent free-field transfer function at any interaction node can be defined by:

$$\tilde{H}_k^{g,i}(\omega) = S_k(\omega)H_k^{g,c}(\omega) \quad (5)$$

where  $S_k(\omega)$  is a frequency-dependent quantity that includes the effects of the stochastic spatial variation of free-field motion at any interaction node dof k due to incoherency.

In fact, in the numerical implementation based on the complex frequency approach,  $S_k(\omega)$  represents the complex Fourier transform of relative spatial random variation of the motion amplitude at the interaction node dof k due to incoherency. Since these relative spatial variations are random,  $S_k(\omega)$ , is stochastic in nature. The stochastic  $S_k(\omega)$  can be com-

puted for each interaction node dof k using spectral factorization of coherency matrix computed for all SSI interaction nodes.

For any interaction node dof k, the stochastic spatial motion variability transfer function  $\tilde{H}_k^{g,i}(\omega)$  in complex frequency domain is described by the product of the stochastic eigen-series expansion of the spatial incoherent field times the deterministic complex coherent ground motion transfer function:

$$\tilde{H}_k^{g,i}(\omega) = \left[ \sum_{j=1}^M \Phi_{j,k}(\omega)\lambda_j(\omega)\eta_{\theta_j}(\omega) \right] H_k^{g,c}(\omega) \quad (6)$$

where  $\lambda_j(\omega)$  and  $\Phi_{j,k}(\omega)$  are the j-th eigenvalue and the j-th eigenvector component at interaction node k. The factor  $\eta_{\theta_j}(\omega)$  in equation 6 is the random phase component associated with the j-th eigenvector that is given by  $\eta_{\theta_j}(\omega) = \exp(i\theta_j)$  in which the random phase angles are assumed to be uniformly distributed over the unit circle,  $\theta_j(\omega) \sim U[-\pi, \pi]$ .

The number of coherency matrix eigenvectors, or incoherent spatial modes, could be either all modes or a reduced number of modes M depending on the eigen-series convergence.

Let's consider now the structural SSI response.

For a coherent motion input, assuming a number of interaction nodes equal to N, the complex Fourier SSI response at any structural dof i,  $U_i^{s,c}(\omega)$ , is computed by the superposition of the effects produced by the application of the coherent motion input at each interaction node k:

$$\begin{aligned} U_i^{s,c}(\omega) &= \sum_{k=1}^N H_{i,k}^s(\omega)U_k^{g,c}(\omega) \\ &= \sum_{k=1}^N H_{i,k}^s(\omega)H_k^{g,c}(\omega)U_0^g(\omega) \end{aligned} \quad (7)$$

where the  $H^s(\omega)$  matrix is the structural complex transfer function matrix given unit inputs at interaction node dofs. The component  $H_{i,k}^s(\omega)$  denotes the complex transfer function for the i-th structural dof if a unit amplitude motion at the k-th interaction node dof is applied. For incoherent motion input, the complex Fourier SSI response at any structural dof i,  $U_i^{s,i}(\omega)$ , is computed similarly by the superposition

of the effects produced by the application of the incoherent motion input at each interaction node dof k:

$$U_i^{s,i}(\omega) = \sum_{k=1}^N H_{i,k}^s(\omega) U_k^{g,i}(\omega) = \sum_{k=1}^N H_{i,k}^s(\omega) \left[ \sum_{j=1}^M \Phi_{j,k}(\omega) \lambda_j(\omega) \eta_{\theta_j}(\omega) \right] H_k^{g,c}(\omega) U_0^g(\omega) \quad (8)$$

Obviously that in equation 8,  $H_{i,k}^s(\omega)$  is the same as in equation 7, since the structural transfer matrix does not depend on seismic input motion characteristics.

Since the implementation uses equation 6 that is derived in free-field before the SSI analysis is started, the number of extracted coherency matrix eigenvectors, or incoherent spatial modes, can be as large as is desired by the user with a very negligible impact on the SSI analysis run time. By default, all the incoherent spatial modes are included. Consideration of all incoherent spatial modes improves the incoherent SSI accuracy and produces a very accurate recovery of the free-field coherency matrix at interaction nodes; this can be checked by the user for each calculation frequency.

The stochastic simulation approach equations 4 and 6 to generate random incoherent input free-field motions. Using Monte Carlo simulation, a set of random incoherent motion samples are generated at interaction nodes. These incoherent motion random samples are obtained by simulating random phase angles in equation 6. For each incoherent motion random sample an incoherent SSI analysis is performed. Finally, the mean SSI response is computed by statistical averaging of the response quantities of interest. Thus, the stochastic simulation approach implies that a set of statistical incoherent SSI analyses are required. The final mean SSI response is obtained by statistical averaging of SSI response random samples.

To speed up the set of SSI simulations, a fast restart option for reanalysis was introduced. This restart option bases on the fact that for each incoherent motion SSI run only seismic load vector changes, while the soil impedance matrix and the structural transfer functions with respect to interaction node excitations remain the same. If the restart option is used the run time for each SSI analysis drops to only 1/3 to 1/5 of the initial run time. Thus, it is possible to do up to 5 stochastic SSI simulations in the time of a single in-

itiation SSI analysis run. This provides quite reasonable run times for the stochastic simulation approach.

The deterministic approach is a fast incoherent SSI analysis approach that approximates the mean SSI response using a *single* SSI analysis run. However, the deterministic approach accuracy is limited to rigid foundation situations as explained hereafter.

The deterministic approach (called in EPRI studies AS (from algebraic sum) is based on a simple, engineering practical rule that has been often accepted in the engineering analysis practice for NPP Seismic PRA reviews, namely that “Median Input produces Median Response”.

The validity of the deterministic approach based on the simple rule “median input provides median output” was investigated in two recent EPRI studies (Short, Hardy, Mertz and Johnson, 2007). It was concluded that for nuclear structural models with rigid mats, the deterministic approach provides very close results for mean SSI response to a rigorous stochastic analysis.

The two EPRI studies also investigated the statistical variation of SSI responses and the statistical convergence of the stochastic simulation approach. It was shown that the use of only five stochastic simulation samples provides a reasonably accurate prediction of the mean SSI responses.

To implement the “median input produces median output” rule for incoherent SSI analysis, AS combines the incoherent spatial modes using a linear algebraic summation as described in equation 6 assuming zero random phase values (the zero phases are the statistical mean phase values). For AS equation 6 simplifies to the following form:

$$\tilde{H}_k^{g,i}(\omega) = \left[ \sum_{j=1}^M \Phi_{j,k}(\omega) \lambda_j(\omega) \right] H_k^{g,c}(\omega) \quad (9)$$

Equation 9 shows that as the result of assuming zero phase angles, the incoherent spatial modes are scaled deterministically by the values of the square roots of the coherency matrix eigenvalues that are also equal to the standard deviations of the spatial modes that are measures of their contributions to the total motion spatial variability.

As a consequence on the zero phase assumption, the deterministic approach is capable to reproduce exactly the free-field coherency matrix if all spatial modes are employed (assuming that no numerical errors occur in the calculation of the eigenvectors of coherency matrix).

### 3 ILLUSTRATIVE APPLICATIONS

Currently, the above described seismic incoherent SSI approaches are employed in several industry projects for evaluating the seismic SSI response of the different nuclear reactor facilities, including the new Westinghouse AP1000 nuclear power plant (Short, Hardy, Mertz and Johnson, 2007, Ghiocel et al., 2009).

Several plane-wave motion incoherency models were considered: i) the Luco-Wong anisotropic wave incoherency model (Luco and Wong, 1986) and, ii) the Abrahamson isotropic wave incoherency models, available for different soil conditions (Abrahamson, 2005, 2006, 2007). In the investigated case studies, the computed incoherent SSI responses are compared with coherent SSI responses to illustrate the effects of motion incoherency on seismic structural response. The SSI results in terms of transfer functions, acceleration response spectra and structural forces are obtained to study incoherency effects.

#### 3.1 Axisymmetric Reactor Building Example

A reactor building with axisymmetric Containment Shell (CS) and Internal Structure (IS) was considered using a Luco-Wong incoherency model. The coherence parameter was assumed to be 0.10. The soil was modeled as a viscous elastic half-space with a  $V_s = 1000$  fps. No wave passage was considered.

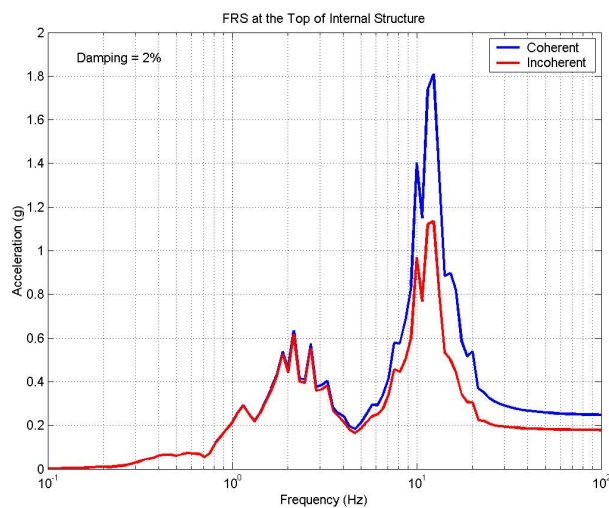


Figure 1. Coherent vs. Incoherent ISRS at Top of IS

The deterministic approach was employed to compute motion incoherency effects. The computed coherent and incoherent acceleration in-structure response spectra (ISRS) at the top of internal structure (IS) and top of containment shell (CS) are compared in Figures 1 and 2.

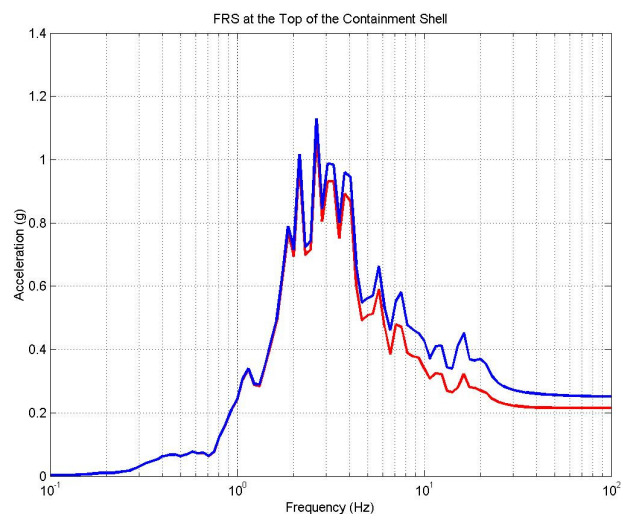


Figure 2. Coherent vs. Incoherent ISRS at Top of CS

The incoherent SSI analysis results indicate a significant reduction of ISRS in higher frequency ranges, although the incoherency effects for a 0.10 coherence parameter are reduced. These results indicate that there is a significant reduction of the ISRS due to motion incoherency effects.

#### 3.2 Nuclear Complex Building Example

This example illustrates the effects of motion incoherency for a nuclear complex building founded on a rock site. In addition to the two EPRI studies (Short, Hardy, Mertz and Johnson, 2006, 2007) that investigated a nuclear complex building using a multiple stick model with a perfectly rigid basemat, herein we consider a detailed finite element structural model with a flexible basemat.

The seismic input motion is very rich in high-frequency components. The 2007 Abrahamson incoherency model that is applicable to rock site conditions was applied. No wave passage was considered. The results of stochastic approach were based on statistical averaging of a set of random realizations.

It should be noted that for flexible foundations, the incoherency-induced stochasticity of the basemat motion is driven by the local spatial variations (point

variations) of free-field motion and, therefore, is much more complex and random, with an unsmoothed spatial variation pattern (kinematic SSI is reduced, so differential free-field motions are less constrained by the basemat). For rigid foundations the incoherency-induced stochasticity of the basemat motion is driven by the global or rigid body spatial variations (integral variations) of free-field motion and, therefore, is less complex and random, with a smoothed spatial variation pattern (kinematic SSI interaction is large, so differential free-field motions are highly constrained by the rigid basemat). Therefore, herein we employed the stochastic incoherent SSI approach.

lear complex building. In these figures we compared the (deterministic) coherent SSI response with the individual, stochastic incoherent SSI responses and with the mean incoherent SSI response.

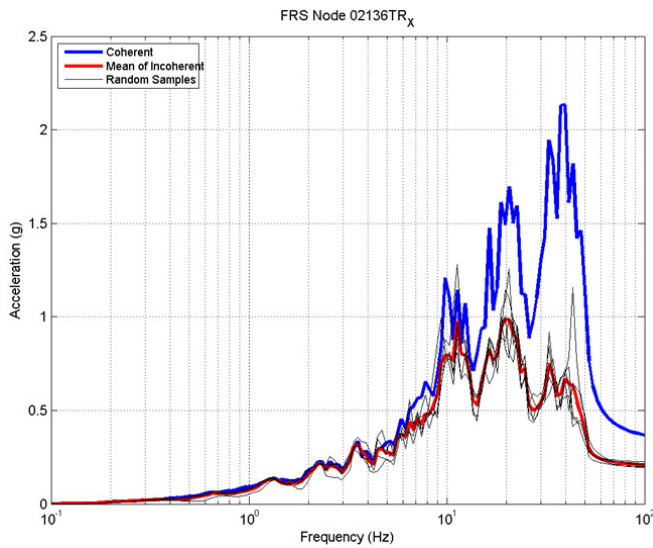


Figure 3. Incoherent vs. Coherent ISRS in X-Direction at Lower Elevation for 3D Input in X, Y and Z Directions

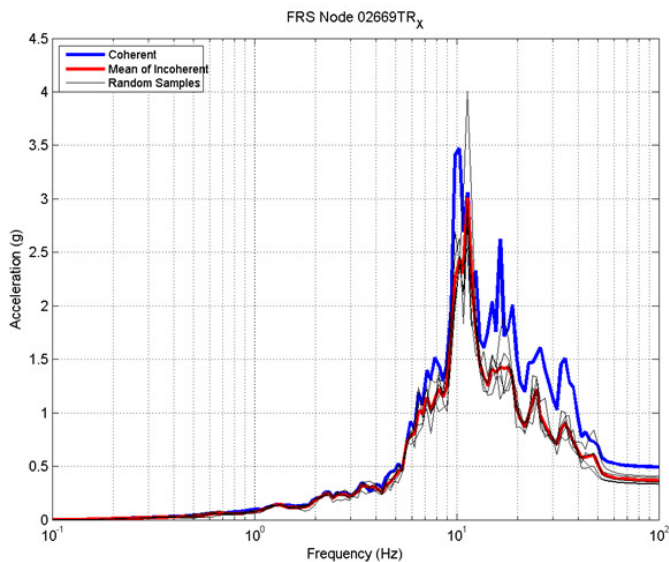


Figure 4. Incoherent vs. Coherent ISRS in X-Direction at Higher Elevation for 3D Input in X, Y and Z Directions

Figures 3 through 6 show the computed ISRS in the X and Z directions at two locations within the nuc-

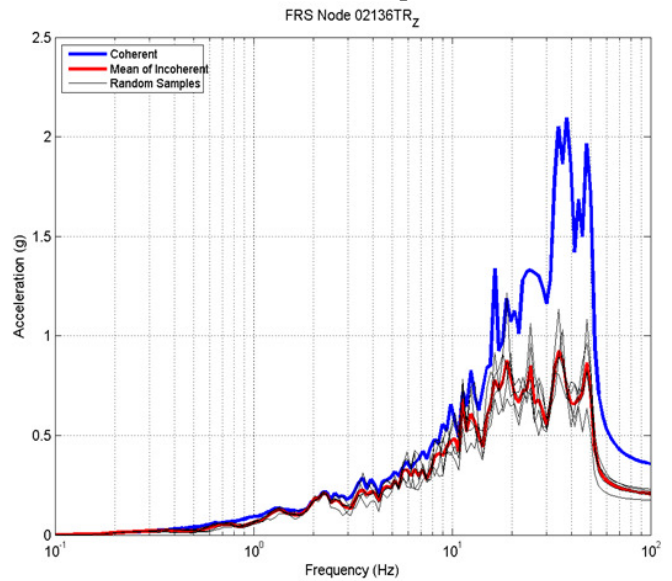


Figure 5. Incoherent vs. Coherent ISRS in Z-Direction at Lower Elevation for 3D Input in X, Y and Z Directions

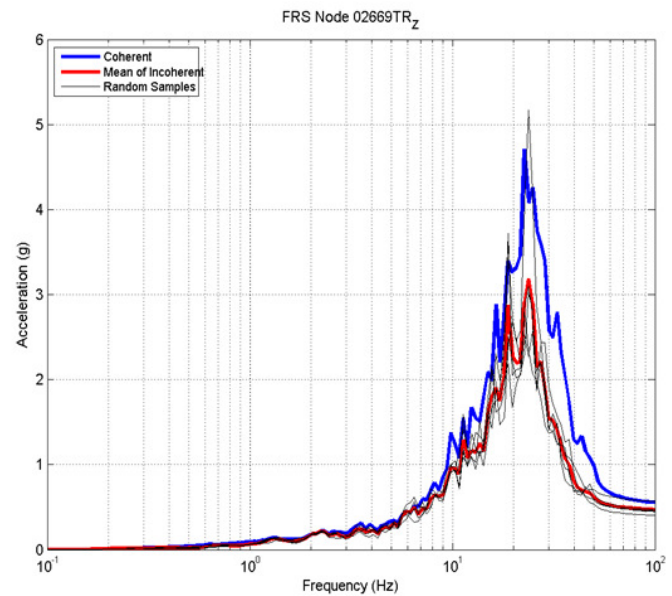


Figure 6. Incoherent vs. Coherent ISRS in Z-Direction at Higher Elevation for 3D Input in X, Y and Z Directions

These figures provide an useful information on the stochasticity of computed FRS due the motion incoherency effects. It should be noted that ISRS stochasticity diminishes for higher elevations.

The coefficients of variation of FRS vary between about 5% (high elevations) to up about 20% (ground elevations). It should be also noted that the ISRS amplitude has a skewed probability distribution, i.e. lognormal could be a good approximation. Thus,

few samples could have much larger spectral peaks than the others, especially at lower elevations where the frequency content of motions has a broader frequency band.

As expected, the mean incoherent ISRS is much lower than the coherent ISRS, especially in the high-frequency range above 20 Hz. Figures 7 and 8 show the mean incoherent ISRS and mean-plus/minus one standard deviation ISRS at a higher elevation for only 5 random SSI simulations. Both ISRS in X and Z directions are shown.

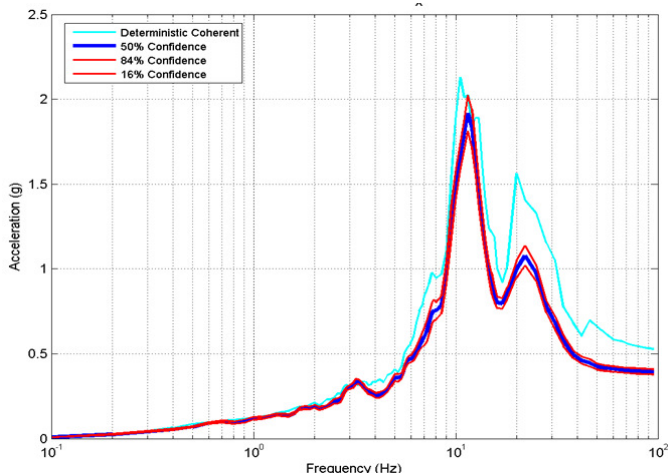


Figure 7 Incoherent vs. Coherent ISRS in X Direction at Higher Elevation for 5 Stochastic Samples

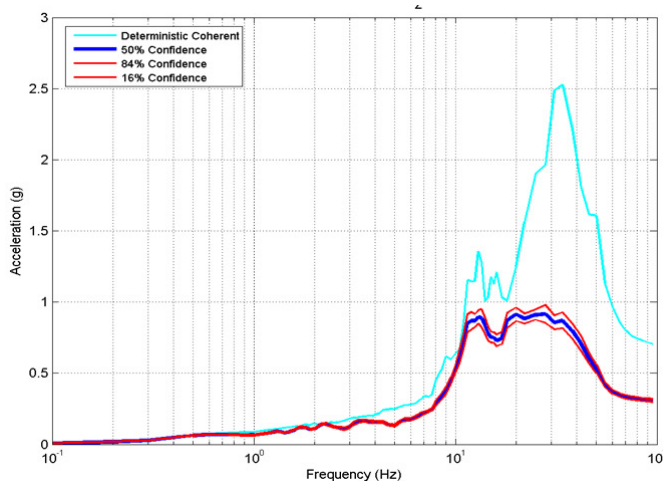


Figure 8 Incoherent vs. Coherent ISRS in Z Direction at Higher Elevation for 5 Stochastic Samples

It should be noted that the relative statistical convergence error expressed by the coefficients of variation of the estimate of the mean ISRS computed for only 5 simulations is relatively small at the basemat level (about 10 percents for a 70%-80% confidence level) and practically negligible at higher elevations (about 5 percents for a 70%-80% confidence level). The

above observation is valid for both the SSI response in X and Z directions.

It should be noted that the relative statistical errors for the mean FRS computed using only 5 simulations appear to be about the same magnitude with the numerical inaccuracies coming from the complex TF interpolation scheme used herein for computing the complex response at 2368 Fourier frequencies based on the computed TF at 220 selected frequencies. Therefore, it appears as a rationale to include interpolation modeling error by performing additional runs with different interpolation options and then, average the results. These additional runs have a totally negligible impact on the overall SSI analysis run time.

It should be also noted, that in comparison with the axisymmetric RB for which the incoherent ISRS were lower than coherent ISRS for all frequencies, for the nuclear complex with mass eccentricities, the incoherent ISRS can be higher than the coherent ISRS for frequencies that correspond to torsional SSI modes for horizontal inputs and rocking SSI modes for vertical inputs.

#### 4 CONCLUDING REMARKS

Based on the investigated case studies, the qualitative effects of motion incoherency effects are as follows: i) for horizontal components a reduction in excitation translation along the input direction concomitantly with an increase in torsional excitation and a slight reduction in foundation rocking excitation, and ii) for vertical component a reduction in excitation translation in vertical direction concomitantly with an increase of rocking excitation. Typically, the effect on motion incoherency is highly beneficial since reduces the seismic ISRS for high-frequency seismic inputs, particularly for rock sites.

For *rigid foundations* the incoherency-induced stochasticity of the basemat motion is driven by the global or rigid body spatial variations (integral variations) of free-field motion and, therefore, is less complex and random than free-field motion. The rigid foundation motion has a smoothed spatial variation pattern since the kinematic SSI interaction is large. Thus, the differential free-field motions are highly constrained by the rigid basemat, and because of this they reduce the pattern complexity of the local motion spatial stochasticity.

For *flexible foundations*, the incoherency-induced stochasticity of the basemat motion is driven by the

local spatial variations of free-field motion and, therefore, is more complex and random, following closely the free-field motion pattern. The flexible foundation motion has a less smoothed spatial variation pattern since kinematic SSI is reduced. Thus, the differential free-field motions are less constrained by the basemat, and because of this they maintain the pattern complexity of the local motion spatial stochasticity.

To accurately capture the statistical nature the local spatial variations of the incoherent motion that are directly transmitted into the flexible basemat motion, we suggested the application of the stochastic incoherent SSI approach, i.e. Simulation approach in EPRI studies.

Based on EPRI studies (Short, Hardy, Mertz and Johnson, 2006, 2007) and our in-house investigations, we recommend the application of the stochastic incoherent SSI approach for SSI models with both rigid and flexible foundations. The stochastic approach is highly accurate and relatively fast since it bases on quick SSI reanalyses.

The two deterministic incoherent SSI approaches, AS or SRSS used in the EPRI studies (Short, Hardy, Mertz and Johnson, 2006, 2007), could be applied to rigid foundations only as described in the conclusions of the last EPRI report. As demonstrated by the EPRI results, these two deterministic incoherent SSI approaches provide slightly conservative results for rigid foundations, more visible for incoherent SSI motions in vertical direction (Ghiocel, 2007).

We recommend the following:

- 1) Use the stochastic approach with at least five simulations. However, if only five samples are considered, then, for such small sample sizes, attention should be given to avoid the strong influences from “outliers”. In addition, we suggest the use of some simple screening criteria to ensure that there is no significant bias included.
- 2) To capture the modeling error produced by the interpolation scheme used for complex transfer function calculations, we suggest considering additional runs with different transfer function interpolation selections. Averaging SSI responses from these additional runs avoids potential numerical inaccuracies due to the selection of SSI frequen-

cies or due to interpolation modeling error in transfer function calculations. Such additional runs have a negligible impact on the overall SSI analysis run time.

The above conclusions add to the conclusions of the EPRI studies (Short, Hardy, Mertz and Johnson, 2006, 2007) that investigated the seismic motion incoherency effects on the SSI response of an AP1000-based multiple stick model with a rigid basemat. In the EPRI studies the effect of foundation flexibility was not considered. Currently, we investigate the effect of motion incoherency for embedded foundations.

#### 4 REFERENCES

- Abrahamson, N. 2005. Spatial Coherency for Soil-Structure Interaction, Electric Power Research Institute, TR 1012968, Palo Alto, CA. December.
- Abrahamson, N. 2006. Program on Technology Innovation: Spatial Coherency for SSI, EPRI Palo Alto, CA, Report 1014101, December.
- Abrahamson, N. 2007. Hard Rock Coherency Functions Based on Pinyon Flat Data, April.
- Ghanem, R.G. and Spanos, P.D..1991. Stochastic Finite Elements: A Spectral Approach, Springer- Verlag.
- Ghiocel, D.M. 2007. Stochastic and Deterministic Approaches for Incoherent Seismic SSI Analysis as Implemented in ACS SASSI Version 2.2, Appendix C, EPRI Palo Alto, CA, Report No. TR-1015111, November
- Ghiocel, D.M., Li, D., Coogler, K. and Tunon-Sanjur, L. 2009. Seismic Motion Incoherency Effects for AP1000 Nuclear Island Founded on Rock Site, submitted to the 20<sup>th</sup> SMiRT Conference, Division K, Osaka, September.
- Short, S.A., G.S. Hardy, K.L. Merz, and J.J. Johnson 2006. Program on Technology Innovation: Effect of Seismic Wave Incoherence on Foundation and Building Response, EPRI Palo Alto, CA, TR-1013504, December.
- Short, S.A., G.S. Hardy, K.L. Merz, and J.J. Johnson. 2007. Validation of CLASSI and SASSI to Treat Seismic Wave Incoherence in SSI Analysis of Nuclear Power Plant Structures, EPRI Palo Alto, CA, TR-1015110, November.
- Tseng and Lilhanand.1997. Soil-Structure Interaction Analysis Incorporating Spatial Incoherence of Ground Motions, Electric Power Research Institute, Palo Alto, CA, Report No. TR-102631 2225.

Vanmarcke, E. 1983. Random Fields, MIT Press.